ORIGINAL ARTICLE

Ugai Watanabe · Misato Norimoto · Minoru Fujita
Joseph Gril

Transverse shrinkage anisotropy of coniferous wood investigated by the power spectrum analysis*

Abstract The transverse shrinkage behavior of early wood and late wood tracheids of radiata pine (*Pinus radiata* D. Don) was investigated by the power spectrum analysis. The representative cell model shapes before and after shrinkage constructed by the analysis revealed that the early wood tracheid showed anisotropic shrinkage, although the late wood tracheid showed almost isotropic shrinkage. To link the macroscopic shrinkage of coniferous wood with the results obtained by the power spectrum analysis, a two-layer model composed of early wood and late wood was adopted, and the relation between shrinkage anisotropy and late wood fraction was predicted. The results suggested that the shrinkage anisotropy depended significantly on the mechanical interaction between early and late wood.

Key words Radiata pine · Cell shrinkage · Shrinkage anisotropy · Power spectrum analysis · Two-layered model

Introduction

The shrinkage anisotropy of coniferous wood in the transverse direction is believed to be affected by the arrange-

U. Watanabe (✉) · M. Norimoto
Laboratory of Property Enhancement, Wood Research Institute,
Kyoto University, Gokasyo, Uji 611, Japan
Tel. +81-774-38-3658; Fax +81-774-38-3600
e-mail: uwatanab@kuwri.kyoto-u.ac.jp

M. Fujita
Division of Forest and Biomaterials Science, Graduate School of
Agriculture, Kyoto University, Kitashirakawa-Oiwake-cho,
Sakyo-ku, Kyoto 606-01, Japan

J. Gril
Laboratoire de Mécanique et Génie Civil, Université Montpellier 2,
UM2-LMGC/bois, CP 81, Place Eugene Bataillon, 34095 Montpellier
Cedex 5, France

ment and transverse shapes of tracheids. It is well known that the separated early wood shows anisotropic shrinkage, whereas the separated late wood shows comparatively isotropic shrinkage.[1,2] Coniferous wood from tropical regions without distinct growth rings also shows anisotropic shrinkage. The effect of cellular structure on shrinkage anisotropy in wood has been investigated through microscopic observations and theoretical approaches using cell models.[3] The causes of anisotropic shrinkage are not always clear. An analysis using a representative cell model would be useful for investigating the shrinkage anisotropy of wood, but it is difficult to establish such a model as there is relatively wide variation in the cellular structure of wood.

Maekawa et al.[4] have applied a two-dimensional power spectrum analysis to the determination of the anatomical features in the transverse section of wood. They quantitatively determined the cell arrangement, which had been qualitatively recognized by microscopic observations. Furthermore, this analysis was utilized to investigate the shrinkage behavior of tracheids.[5] The shrinkage of a representative model of coniferous wood agreed well with macroscopic shrinkage.

These results suggested that the power spectrum analysis can effectively clarify the relation of cellular structures to macroscopic shrinkage of coniferous wood. In this study, the transverse shrinkage behavior of early and late wood tracheids of radiata pine were investigated using the power spectrum analysis. A two-layered model composed of early wood and late wood was chosen to link the macroscopic shrinkage of coniferous wood with the results obtained by the power spectrum analysis, and the relation between transverse shrinkage anisotropy and late wood fraction was investigated.

Materials and methods

Radiata pine (*Pinus radiata* D. Don) with an air-dried density of $0.41\,g/cm^3$ and an average annual ring width of 15 mm was used. Specimens for measurement of shrinkage and Young's modulus were prepared from the same block. As

shown in Fig.1, five early wood specimens [A: 5mm (R) × 5mm (T) × 40mm (L)], five late wood specimens [B: 5mm (R) × 5mm (T) × 40mm (L)] and ten specimens containing late wood and early wood [C: 30mm (R) × 30mm (T) × 5mm (L)] were prepared from the wood block (R, radial; T, tangential; L, longitudinal). Lines along the radial and tangential directions were drawn on the transverse surface of specimen C to measure shrinkage. All specimens were soaked in distilled water until saturated. The transverse surfaces of specimens A and B in the wet condition were smoothed by a sliding microtome.

Construction of cell model shape

After all surfaces of specimen A, except the one to be replicated, had been sealed with a thin polyvinylidene chloride film to avoid water evaporation, the specimen was a pressed against polyethylene film (0.1mm thickness) softened by heating at about 130°C on a glass slide to obtain a replica.[6] The specimen was dried slowly at room temperature for 5 days, placed in a closed chamber conditioned at 98% relative humidity (RH) for 5 days, dried over P_2O_5 at 60°C, and finally dried overnight at 105°C. A replica under oven-dried conditions was then obtained. The late wood portion of specimen B was separated using a razor. Replicas under both conditions were obtained in the same manner.

Light micrographs were obtained at three positions on the replicas prepared under wet and oven-dried conditions. Cell matrices of 15 × 15 were set up on the micrographs. The edges between walls and lumens in the matrices were traced on a clear sheet. The traced figures were then input into an image analyzing system (Luzex III) using a television camera so the radial direction of figures coincided with the axial direction of the monitor, smoothed and converted to binary figures. The center of gravity for each cell was
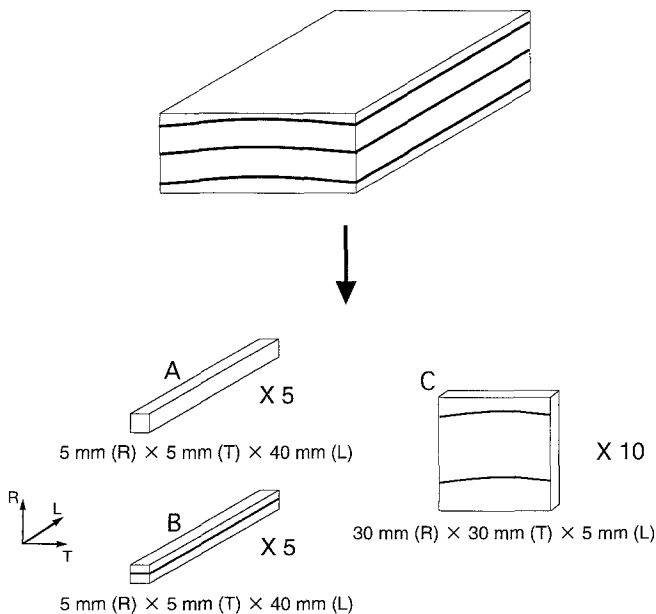
Fig. 1. Preparation of specimens for measuring shrinkage. R, radial direction; T, tangential direction; L, longitudinal direction

derived from the binary figures and was shown by a dot (diameter 7 pixels) on the monitor. After the dots and background were converted to a gray-level image of 255 and 0, respectively, a fast Fourier transform (FFT) was conducted to obtain a power spectrum.

The periodicity of the cell arrangement was determined from the power spectrum as follows[4]: A set of dots is mathematically expressed by the following function $D(s, t)$ which convolutes the delta functions of cell positions $\delta(s - x_i, t - y_i)$ and the aperture function of a dot $A(s, t)$.

$$D(s, t) = A(s, t) * \{\delta(s - x_1, t - y) + \ldots \delta(s - x_N, t - y_N)\}$$

(1)

where x_i and y_i are coordinates of the ith dot, and $*$ is an operator of convolution. By the Fourier integration of $D(s, t)$, the power spectrum of the delta functions in polar coordinates (k, φ) is given by

$$P_\delta(k, \varphi) = \frac{1}{2} \sum_{i=2}^{N} \sum_{j=1}^{N} 2 \cos \frac{2\pi k \{(x_i - x_j) \cos\varphi (y_i - y_j) \sin\varphi\}}{M} + N$$

$$(i \neq j)$$

(2)

where k is the frequency, and M is the size of the monitor (1024 in this case). This equation represents the Fourier transform of all dots projected on a line in the φ direction. The periodicity of cell position in the radial direction ($\varphi = \pi/2$) and the periodicity of radial files in the tangential direction ($\varphi = 0$) were determined from this equation.

The direction of cell arrangement can be estimated from the power density at each angle for Eq. (2), namely,

$$p_\delta(\varphi) = \frac{1}{2} \sum_{i=1}^{N} \sum_{j=1}^{N} \int_{k_1}^{k_2} \left[2 \cos \frac{2\pi k \left\{ \begin{array}{c} (x_i - x_j) \cos\varphi \\ + (y_i - y_j) \sin\varphi \end{array} \right\}}{M} + N \right] dk$$

(3)

The power density of each angle at a low frequency band of 30–100 pixels was adapted to determine the direction of the cell arrangement. The density was obtained by reading and integrating the gray levels of the power spectrum image using a computer.

To investigate the cell wall orientation in the transverse direction, the cell wall regions between adjacent lumens in the figure input were painted by the computer, and a figure of the central line of the cell walls was created by thinning the thickness to 1 pixel. This figure was converted to a gray-level image and subjected to FFT to obtain a power spectrum, which was saved on a floppy diskette. The power spectrum of the image consisting of the rectangular elements with length L, width B, and weight per unit area m is expressed by

$$P_r(k, \theta) = \frac{1}{\eta \overline{m}^2} \int_m \int_0^{2\pi} m^2 \operatorname{sinc}^2 \{\pi k L \cos(\theta' - \theta)\}$$

$$\cdot \operatorname{sinc}^2 \{\pi k B \sin(\theta' - \theta)\} \cdot H(m, \theta') d\theta' dm$$

(4)

where h and $\bar{m}$ are the number of elements and the weight per unit area of the image, respectively, and $H(m, \theta')$ is the function expressing the relation between m and the longitudinal direction of an element θ'.[7] The orientation of elements can be estimated by the power spectrum density at each angle:

$$p_r(\theta) = \int_{k_1}^{k_2} P_r(k,\theta)dk \tag{5}$$

The following relation is confirmed by a numerical analysis.

$$p_r(\theta + \pi/2) = \int_m H(m,\theta)dm \tag{6}$$

The orientation of the cell wall was estimated by regarding the figure made by thinning the cell walls as consisting of rectangular elements. The power density of each angle at a higher frequency band of 200–300 pixels was adapted to determine the orientation of the cell wall. The density was obtained by reading and integrating the gray levels of the power spectrum image using a computer.

The cell model shape was constructed as follows. Cell positions were determined from the periodicities and directions of the cell arrangement. A cell element was placed at an angle determined from Eq. (6) in the middle of two cell positions. All cell elements were connected to construct the model shape, as shown in Fig. 2.
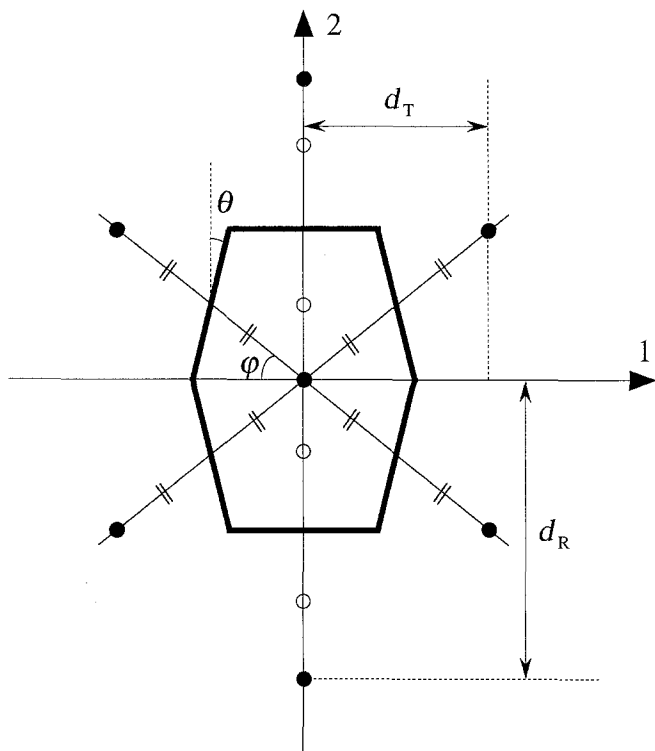
Fig. 2. Transverse cell model shape constructed by the power spectrum analysis. d_T, d_R, tangential and radial periodicities of cell position determined by Eq. (2); φ, direction of cell arrangement determined by Eq. (3); θ, direction of cell wall orientation determined by Eq. (6).

Measurement of macroscopic shrinkage and late wood fraction

Specimen C was dried in the manner mentioned above, and the radial and tangential shrinkages were calculated from the dimensional change of the specimen measured by a traveling microscope. The radial width of the darker portion of specimen C was measured by a traveling microscope to determine the late wood fraction.

Measurement of tangential Young's modulus

Two wood blocks containing one annual ring [15mm (R) × 50mm (T) × 100mm (L)] were glued at radial surfaces with polyvinyl acetate adhesive. Ten specimens [15mm (R) × 100mm (T) × 1mm (L)] were prepared from the block to measure the tangential Young's modulus. Ten specimens [10mm (R) × 100mm (T) × 1mm (L)] to measure the tangential Young's modulus of early wood specimen were prepared in the same manner. The measurement was carried out at 20°C and 60% RH by a free – free flexural vibration method. It has been confirmed that the glue line has no influence on the results.[8]

Results and discussion

Shrinkage behavior of early and late wood tracheids

Figure 3 shows the representative cell model shapes of early and late wood tracheids constructed by the power spectrum analysis. The shrinkage determined by the power spectrum analysis for the center of gravity of each cell agreed well with the macroscopic shrinkage, and the features of shrinkage deformation could be expressed well by the models constructed by the analysis.[5]

The representative model of an early wood tracheid of radiata pine had a hexagonal, slightly asymmetrical shape. The cell rotated slightly during drying. The radial and tangential shrinkages of the model were 2.5% and 5.5%, respectively. The axial shrinkages of cell elements a, b, and c were 4.2%, 3.7%, and 6.2%, respectively. The included angles between two radial walls under wet (α) and oven-dried (β) conditions were 128° and 133°, respectively, so the angle increased by 5° during drying. The early wood tracheid itself showed anisotropic shrinkage with changing cell shape, which might cause anisotropic shrinkage in the separated early wood. On the other hand, the transverse shape of late wood tracheids was almost rectangular. The radial and tangential shrinkages of the model were 7.2% and 8.0%, respectively. No rotation of cell shape during drying was observed. The included angle was slightly increased during drying. The axial shrinkages of the cell elements d and e were 7.9% and 7.2%, respectively. Late wood tracheids showed almost isotropic shrinkage.

Different shrinkage behavior was observed between early and late wood tracheids of radiata pine. Therefore
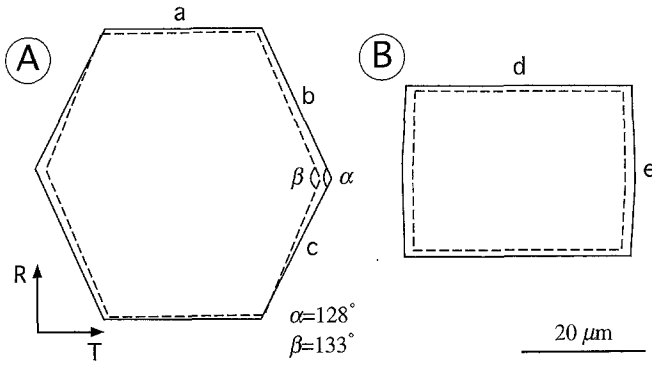
Fig. 3. Cell model shapes under wet (*solid line*) and oven-dried (*dotted line*) conditions for early (**A**) and late (**B**) wood tracheids of radiata pine

Table 1. Experimental values for radiata pine

Tangential shrinkage ε_1 (%)	6.32
Radial shrinkage ε_2 (%)	2.54
Tangential shrinkage of late wood α_1^a (%)	8.01
Tangential shrinkage of early wood α_1^b (%)	5.46
Radial shrinkage of late wood α_2^a (%)	7.23
Radial shrinkage of early wood α_2^b (%)	2.52
Tangential Young's modulus E_1 (GPa)	0.42
Tangential Young's modulus of early wood E_1^b (GPa)	0.37
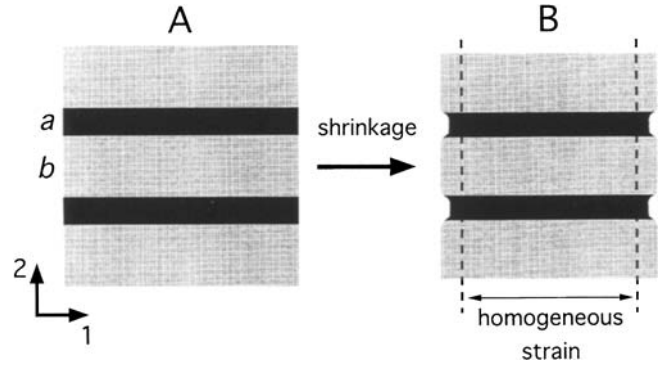
Fig. 4. Coniferous wood model. Layers a and b correspond to late and early wood, and directions 1 and 2 to tangential and radial directions, respectively. A represents wet conditions and B is after drying

when analyzing the shrinkage anisotropy of coniferous wood with a low volume fraction of ray tissue, the mechanical interaction between early and late wood must be taken into consideration.

Shrinkage anisotropy of coniferous wood

Microscopic shrinkage of early and late wood was determined by the power spectrum analysis. The radial and tangential shrinkage and the tangential Young's modulus of whole wood specimens and the tangential Young's modulus of early wood specimens were also measured. The results are shown in Table 1. Using these values, shrinkage of the two-layered model was calculated to investigate the shrinkage anisotropy of coniferous wood.

Figure 4 shows a model of coniferous wood in which layers a and b represent late and early wood, and the directions 1 and 2 correspond to the tangential and radial directions, respectively. Model A under wet condition may change to model B after drying. A homogeneous strain may occur in direction 1 but not in the edge portions in direction 2, as shown in model B. The shrinkages $[\varepsilon_i \ (i = 1, 2)]$ and stresses $[\delta_i \ (i = 1, 2)]$ of the model can be expressed with the shrinkages $[\varepsilon_i^k]$ and stresses $[\delta_i^k \ (i = 1, 2; k = a, b)]$ of early wood and late wood.

$$\varepsilon_1 = \varepsilon_1^a = \varepsilon_1^b \qquad \sigma_1 = \phi\sigma_1^a + \psi\sigma_1^b(=0)$$
$$\varepsilon_2 = \phi\varepsilon_2^a + \psi\varepsilon_2^b \qquad \sigma_2 = \sigma_2^a = \sigma_2^b(=0) \tag{7}$$

where ϕ and ψ $(=1 - \phi)$ are late wood and early wood fractions, respectively. Assuming elastic strains occur in a and b layers due to mechanical interaction during drying, the shrinkages of a and b layers can be expressed by the following equations.

$$\left.\begin{aligned}\varepsilon_1^a &= \frac{1}{E_1^a}\sigma_1^a - \frac{v_{21}^a}{E_2^a}\sigma_2^a + \alpha_1^a \\[2mm] \varepsilon_1^b &= -\frac{v_{12}^b}{E_1^b}\sigma_1^b + \frac{1}{E_2^b}\sigma_2^b + \alpha_1^b\end{aligned}\right\} \tag{8-1}$$

$$\left.\begin{aligned}\varepsilon_2^a &= \frac{1}{E_1^a}\sigma_1^a - \frac{v_{21}^a}{E_2^a}\sigma_2^a + \alpha_2^a \\[2mm] \varepsilon_2^b &= -\frac{v_{12}^b}{E_1^b}\sigma_2^b + \frac{1}{E_2^b}\sigma_2^b + \alpha_2^b\end{aligned}\right\} \tag{8-2}$$

where E_i^k $(i = 1, 2; k = a, b)$ are the elements of the matrix and α_i^k $(i = 1, 2; k = a, b)$ are the shrinkages of layers. From these equations, ε_1 and ε_2 are given by

$$\varepsilon_1 = \lambda\alpha_1^a + (1 - \lambda)\alpha_1^b \tag{9-1}$$

$$\varepsilon_2 = \phi\alpha_2^a + \psi\alpha_2^b + C \tag{9-2}$$

$$E_1 = \phi E_1^a + \psi E_1^b \tag{9-3}$$

where λ and C are $\phi E_1^a/E_1$ and $(\alpha_1^b - \alpha_1^a)\{\psi v_{12}^b\lambda - \phi v_{12}^a (1 - \lambda)\}$, respectively. The Poisson's ratios for late and early wood portions, v_{12}^a and v_{12}^b (the ratio of the strain in the direction 1 to that in the direction 2), are required to calculate the shrinkage in the direction 2. Generally, the Poisson's ratio of cellular solids can be determined by geometrical calculation of the cell shape. Regarding the slightly asymmetrical shape of the early wood tracheid shown in Fig. 3A as a symmetrical one, v_{12}^b was determined by the following expression[9]

$$v_{12}^b = \frac{(a/b + \sin\theta)\sin\theta}{\cos^2\theta} \tag{10}$$

where a/b is the ratio of the axial length of cell element a to that of cell element b. The value of v_{12}^b was calculated to be 0.74. However, this equation cannot provide the Poisson's

ratio of the late wood portion in which tracheids have lower θ values. For convenience, v_{12}^a was assumed to be 0.5.

Substituting the experimental values shown in Table 1 in Eq. (9-1), a value of 0.25 was obtained for ϕ, and a value of 0.57 GPa was estimated for E_1^a. On the other hand, a value of 0.06 was obtained by substituting the values for Eq. (9-2). In this case, a value of 1.20 GPa was estimated for E_1^a. The experimental value of ϕ for specimen C was 0.17. In this case, a value of 0.66 GPa was obtained for E_1^a. There was a difference between ϕ values calculated from Eq. (9-1) and (9-2). This difference was considered to originate in the simple analysis using a two-layer model. However, the experimental values of 0.17 showed an almost middle value between the two calculated values of 0.06 and 0.25. Therefore it was considered that the analysis of transverse shrinkage behavior by the two-layer model was valid as a first approximation.

The shrinkage anisotropy of coniferous wood was predicted from Eq. (9-1) and (9-2) with values of 0.17 and 0.66 GPa for ϕ and E_1^a. Figure 5 shows the relation between tangential shrinkage ε_1 and late wood fraction ϕ. The solid line represents the calculated values, which increased with increasing ϕ. Figure 6 shows the relation between radial shrinkage ε_2 and ϕ. The solid line shows the values calculated by Eq. (9-2), and the dotted line shows the values calculated without the interaction term C. Although both values increased with increasing ϕ, the dotted line increased more rapidly. Figure 7 shows the relation between the shrinkage anisotropy ($\varepsilon_1/\varepsilon_2$) and ϕ. The dotted line decreased more rapidly with increasing ϕ. These results show that the influence of the mechanical interaction on $\varepsilon_1/\varepsilon_2$ is significant.

Because $\psi v_{12}^b \lambda$ was about three times larger than ϕv_{12}^a $(1 - \lambda)$, the effect of $\psi v_{12}^b \lambda$ on C is remarkable.

$$\psi v_{12}^b \lambda = \psi v_{12}^b \frac{\phi E_1^a}{\phi E_1^a + \psi E_1^b}$$

This equation contains early wood fraction (ψ) and the Poisson's ratio of early wood (v_{12}^b), Young's modulus of late
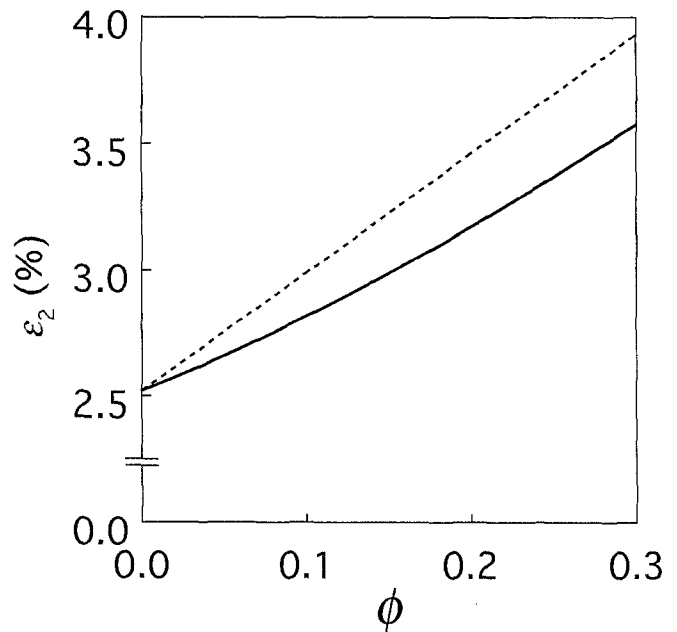
Fig. 6. Relation between calculated values of radial shrinkage (ε_2) and late wood fraction (ϕ). *Solid* and *dotted lines* show the results calculated from Eq. (9-2) and the equation without the interaction term C, respectively

Fig. 5. Relation between calculated values of tangential shrinkage (ε_1) and late wood fraction (ϕ)
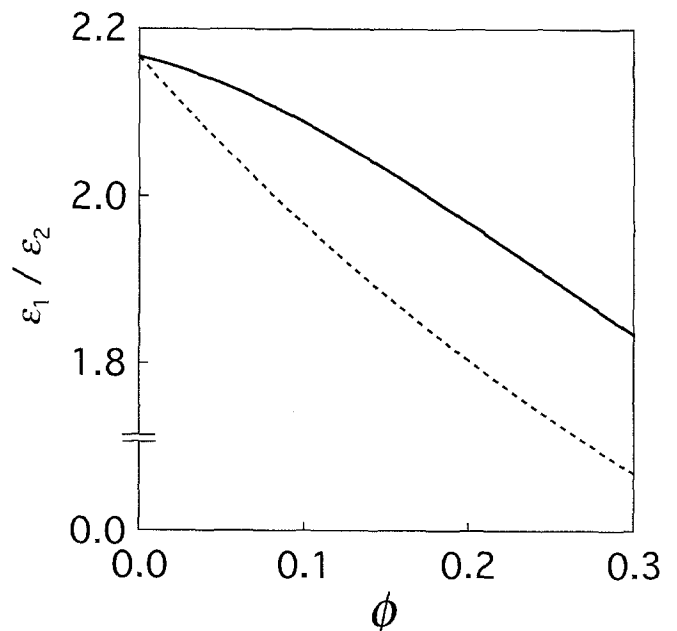
Fig. 7. Relation between shrinkage anisotropy ($\varepsilon_1/\varepsilon_2$) and late wood fraction (ϕ). *Solid* and *dotted lines* show the results calculated with and without the interaction term C, respectively

wood (E_1^a), and Young's modulus of early wood (E_1^b). E_1^a can be regarded as a constant value, because there is almost no difference in the transverse shapes of late wood tracheids among species. Therefore C depends significantly on both v_{12}^b and E_1^b. These results suggest that the shrinkage anisotropy of coniferous wood depends remarkably on the transverse shape of early wood tracheids.

References

1. Pentoney RE (1953) Mechanisms affecting tangential vs. radial shrinkage. J Forest Prod Res Soc 3(2):27–32
2. Nakato K, Kajita S (1955) On the cause of the anisotropic shrinkage and swelling of wood. VI. On the relationships between the annual ring and the anisotropic shrinkage (in Japanese). J Jpn Forest Soc 37(1):22–25
3. Nakato K (1963) Current trends in researches on the mechanism of anisotropic shrinkage of wood (in Japanese). Mokuzai Gakkaishi 9:147–152
4. Maekawa T, Fujita M, Saiki H (1993) Characterization of cell arrangement by polar coordinate analysis of power spectral patterns (in Japanese). J Soc Mater Sci Jpn 42:126–131
5. Watanabe U, Fujita M, Norimoto M (1996) Analysis of the shrinkage deformation of wood cells using the replica and fast Fourier transform methods. In: Donaldson LA, Singh AP, Butterfield BG, Whitehouse LJ (eds) Recent advances in wood anatomy. New Zealand Forest Research Institute Ltd. pp 363–365
6. Adachi A, Ishimaru Y, Fujita M, Sadoh T (1989) Swelling anisotropy of wood in organic liquids. II. Transverse swelling behavior of buna revealed by the replica method (in Japanese). Mokuzai Gakkaishi 35:689–695
7. Yuhara T, Hasuike M, Murakami K (1987) Application of the image processing technique for analysis on sheet structure of paper. III. Determination of the fiber orientation distribution of paper (in Japanese). Jpn Tappi J 41:523–529
8. Yano H, Yamada T (1985) The dynamic mechanical-properties of wood in the radial direction (in Japanese). Mokuzai Gakkaishi 31:222–230
9. Gibson LJ, Ashby MF (1988) The mechanics of honeycombs. In: Cellular solids. Pergamon, Oxford, pp 69–118